Microstructure-Oriented Fatigue Assessment of Construction Materials and Joints Using Short-Time Load Increase Procedure*

Frank Walther, Dortmund, Germany

Stress-strain-hysteresis, change in deformation-induced temperature and change in DC-based electrical resistance measurements are applied for the detailed characterization of structural-mechanical processes in construction materials and joints under multiple-step and single-step fatigue loading. Results concerning the influence of joining technologies on austenitic steel AISI304, carbon-fiber reinforced polymers (CFRP) and beech wood materials, of environmental media on magnesium alloys Mg-4Al-2Ba-2Ca (DieMag422) and Mg-10Gd-1Nd, and of manufacturing processes on titanium alloy Ti-6Al-4V and wood-plastic composites (WPC) are discussed. The load- and cycle-dependent change in microstructure was investigated by light and electron microscopy and correlated with fatigue properties, to reach a preferably precise description of process structure property relationship in a qualitative and quantitative manner. The time-efficient load increase procedure applied for evaluation of joining, environmental and manufacturing influence on fatigue performance is suitable for production-accompanied usage.

Article Information

Correspondence Address
Prof. Dr.-Ing. Frank Walther
Technical University Dortmund
Department of Materials Test Engineering (WPT)
Baroper Str. 303
44227 Dortmund, Germany
E-mail: frank.walther@tu-dortmund.de

Keywords
Materials testing, lightweight alloys, joining technologies, environmental and manufacturing influences, fatigue assessment and calculation

Besides promising part design and application-oriented material selection, the understanding of the fatigue performance of the employed materials and joints is of critical importance for a reliable and economic operation of cyclically loaded components. The fatigue behaviour is very closely related to the microstructure and characterized by the complexity of the interacting operations. Alternating stresses cause micro-plastic deformation in the material and characteristic dislocation structures by cyclic hardening and/or softening mechanisms. These dislocations can be the starting points of a fatigue crack. The fatigue-related property changes lead to crack initiation followed by crack propagation, and ultimately to failure.

Lightweight materials are distinguished by good mechanical properties combined with low density and faces challenges in many areas of new joining technologies. In addition to the systematic microstructure-oriented characterization of the fatigue behaviour, development of application-oriented measurement and analysis methods for component design and operational condition-monitoring with the aim of remaining lifetime assessment is another key area. On the basis of a precise characterization, evaluation and prediction of fatigue mechanisms taking into account the expected load and the corresponding fatigue life, component design can be optimized resulting in a reduction of safety factors. This can increase the ecological and economic performance in the sense of resource-oriented lightweight construction.

Test Method

Physical measurement methods have been employed during the fatigue tests to determine the influence of joining, environment and manufacturing processes on the development of fatigue damage taking the applied loadings into account. The fatigue damage development determined in stepwise and continuous load increase tests serves as a basis for determination of suitable loading parameters in single step tests. The corrosion behaviour of the corrosion-susceptible light metals (aluminium, magnesium) and composites of metals and carbon fiber-reinforced plastics (CFRP)

* Extended Version of the Contribution to the National Conference Werkstoffprüfung 2013

was characterized using electrochemical test systems. The results portray the qualitative and quantitative influence of manufacturing parameters as well as corrosive conditions on the fatigue properties.

Changes in the mechanical material behaviour under cyclic loading are usually described by means of the plastic strain amplitude [1, 2] which is plotted as a function of the number of cycles in cyclic deformation curves. In addition, the change in deformation-induced temperature [3-5] and the change in DC-based electrical resistance [6-9] during the tests have been determined with high accuracy. Besides the geometry the electrical resistance depends on the resistivity which varies with the plastic forming processes due to increased defect density, i. e., micro-cracks, pores. The measurands based on microstructural changes in the material volume are directly related to the current fatigue state. Thus, temperature and resistance measurement methods can be applied for condition monitoring of components and for non-destructive early detection of the damage state of the component in inspection intervals to ensure optimized structural integrity [10-14].

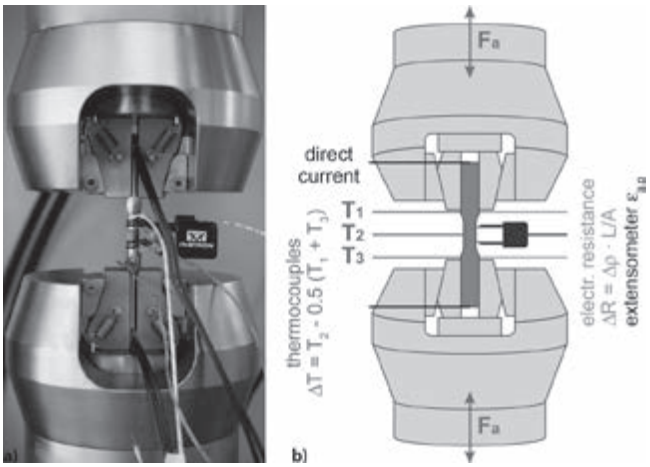

Figure 1. Experimental setup of clamped specimen with applied sensors for fatigue tests in servo-hydraulic testing system, a) Photograph, b) Schematic illustration

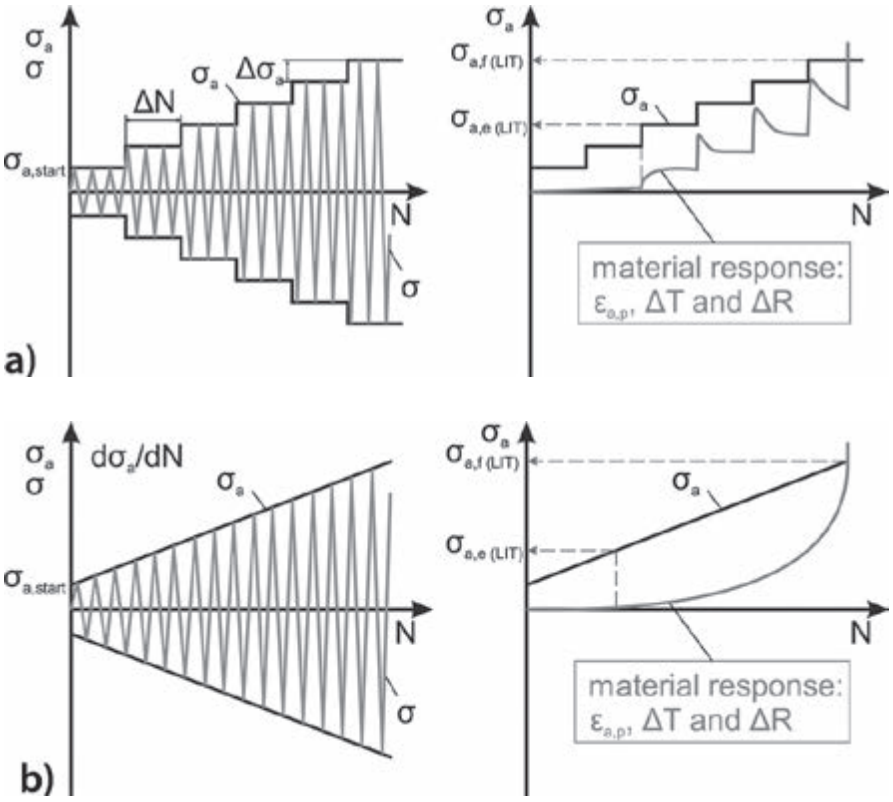

Figure 2. Tests with corresponding material responses as basis for determination of characteristic values, a) stepwise load increase, b) continuous load increase

A representative experimental setup with a round specimen mounted in a servo-hydraulic testing system with applied measurement sensors is illustrated in Figure 1a as photograph and corresponding schematic drawing in Figure 1b.

Stepwise and continuous load increase tests [10-13] were carried out to determine damage and fracture inducing loadings as well as parameter identification for microstructure-correlated single step tests in short time.

In Figure 2 two types of short time load increase tests are illustrated schematically including corresponding material responses. In Figure 2a, the stress amplitude starts at quasi-damage-free level $\sigma_{a,start}$ and is stepwisely increased by $\Delta\sigma_a$ each ΔN cycles until failure. In Figure 2b, the stress amplitude is continuously increased from $\sigma_{a,start}$ by slope $d\sigma_a/dN$ until failure. For both cases of load increase procedure the corresponding material response based on physical measurement techniques, i. e., plastic strain amplitude $\varepsilon_{a,p}$, change in temperature ΔT and change in electrical resistance ΔR, are plotted as cycle- and load-dependent development. The endurance limit $\sigma_{a,e\,(LIT)}$ can be estimated by the determination of the transition from zero values to significantly increasing material response values and the failure stress amplitude $\sigma_{a,f\,(LIT)}$ can be determined as the last loading amplitude at the end of the load increase test (LIT) [11, 14].

One test in load increase mode gives comprehensive information about the cyclic properties and fatigue performance of a material, a material condition, fastenings and joining parameters and processes which have been experimentally validated in single step tests in the high-cycle fatigue (HCF) range up to 2×10^6 or 10^7 load cycles. Due to time- and cost-efficient advantages, the rapid fatigue performance identification method based on combined load increase and few single step tests is suitable for production-accompanied testing in the sense of property-optimized manufacturing of components.

Results

Brazed Joints of Austenitic Stainless Steel AISI 304 and Brazing Alloy BNi-2. Figure 3a represents the results of a stress-controlled stepwise load increase test carried out with a load ratio of R = 0.1 at frequency f = 10 Hz for brazing joint AISI 304/BNi-2. The maximum stress was increased from $\sigma_{max,start}$ = 100 MPa each $\Delta N = 10^4$ cy-

cles by $\Delta\sigma_{max}$ = 10 MPa. The ordinate on the left hand side shows the maximum stress σ_{max} as well as the stress amplitude σ_a. At the load ratio R = 0.1 the relation applies to $\sigma_a = 0.45 \times \sigma_{max} = 4.5 \times \sigma_{min}$ between the stress amplitude, the maximum stress and the minimum stress. The plastic strain amplitude $\varepsilon_{a,p}$ was measured with an extensometer of gauge length L_0 = 10 mm, the change in temperature ΔT with thermocouples fixed in the middle of gauge length of specimen at the brazing seam, and the change in electrical resistance at the transition from gauge length to shafts of specimen [11, 14].

The life-cycle-dependent change in plastic strain amplitude ($\varepsilon_{a,p}$-N) and change in electrical resistance (ΔR-N) are shown as a function of loading amplitudes σ_{max} and σ_a, respectively, and number of load cycles N from 0.5×10^4 onwards. The failure of the brazed AISI 304/BNi-2 joint occurs at σ_{max} = 230 MPa, where the plastic strain amplitude $\varepsilon_{a,p}$ gives an indication only in the last few load cycles. The plotted change in electrical resistance ΔR gives a clearly observable indication of changing fatigue state and impending failure from σ_{max} = 190 MPa onwards. The ΔR change increases to 2 μΩ at load level σ_{max} = 230 MPa, before the final macro-crack propagation increases it exponentially. These information gained by change in electrical resistance measurement could be used for the evaluation of fatigue processes and damage development in brazed joints. Only by combination of novel measurement and testing techniques, in this case high-accuracy DC-based resistance measurements in stepwise load increase tests, the foundation of reliable condition monitoring and structural integrity of fatigue-loaded brazed parts can be guaranteed.

Plotting the change in resistance ΔR as function of the change in temperature ΔT for pair of values of defined load levels of another stepwise load increase test (Figure 3b) reveals interesting features. After an initial approximately linear relation between ΔT and ΔR, the change in electrical resistance changes to exponential increase within the last load levels towards the end of the test. Based on ΔR the critical damage and the failure can be precisely characterized and predicted, since several fatigue mechanisms and defects are integrally included.

Figure 3c shows a cross-section of the brazing joint AISI 304/BNi-2 which was etched for 30 s in a cold etchant for high-alloy steels. Along the brazing seam, an accumulation of dark areas as well as an infil-

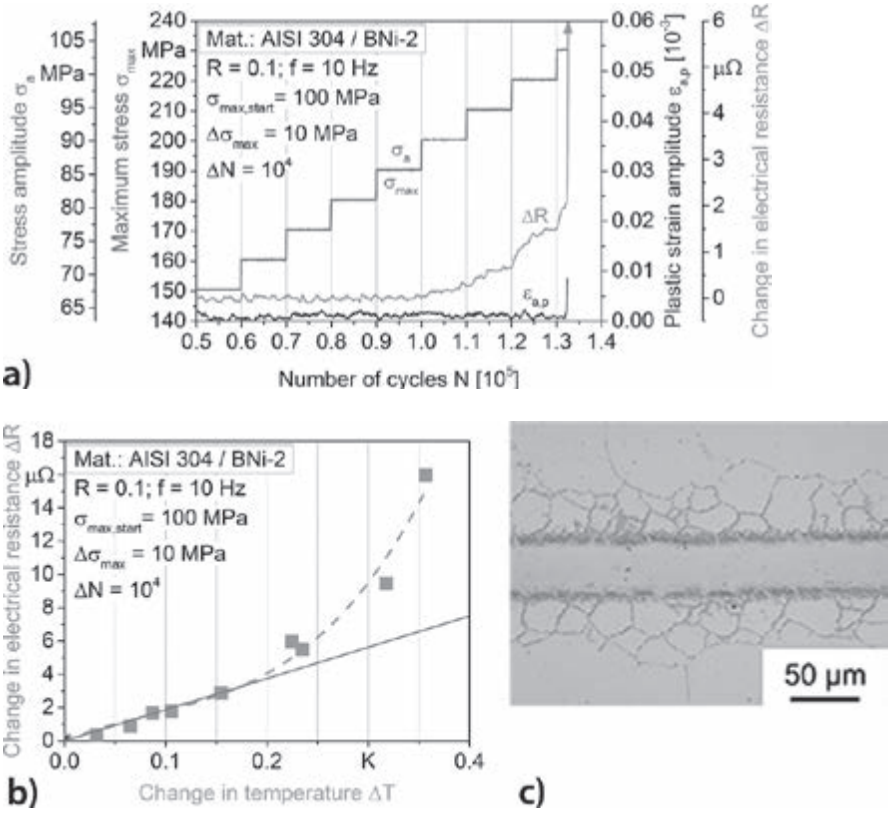

Figure 3. Test results for the AISI 304/BNi-2 brazing joints, a) stepwise load increase test with loading and material reaction values, b) correlation of deformation-induced changes in resistance and temperature, c) microstructural cross-section

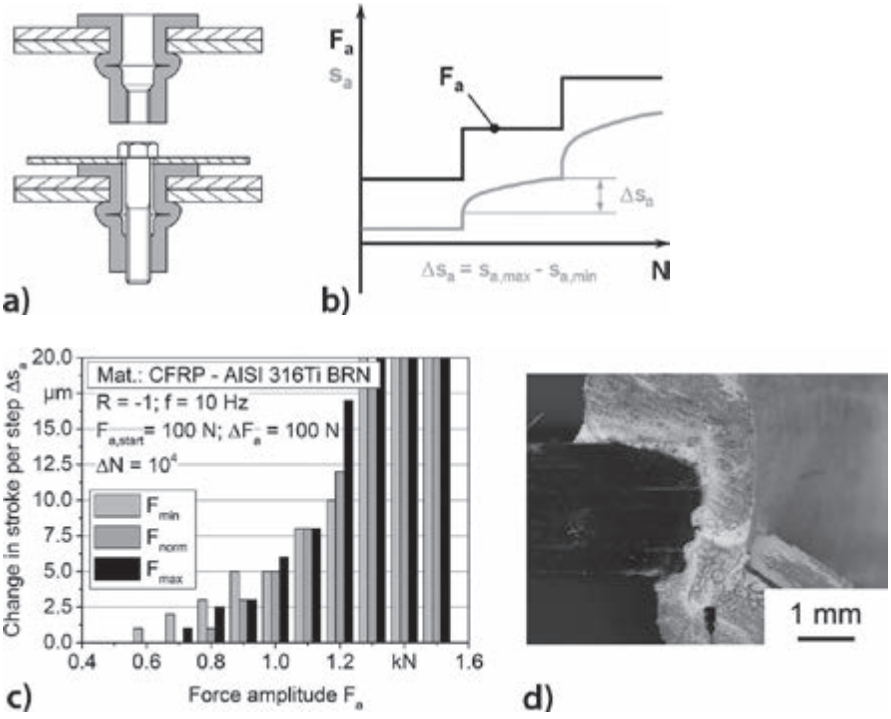

Figure 4. a) Schematic illustration of blind rivet nut compound, b) schematic illustration of stepwise load increase test with measurement of change in displacement, c) change in displacement force amplitude measurement for different plant forces of a CFRP stainless steel compound, d) microstructural cross-section of a CFRP aluminium compound after corrosion treatment

tration of the grain boundaries with components of the brazing alloy can be observed. No brittle phase exists at the centre of the brazing seam.

Fastening of Carbon Fiber-Reinforced Polymer (CFRP) Sheets with Metallic Blind Rivet Nuts. With the objective of ensuring reliable and reproducible production technology, the influence of manufacturing parameters has been studied on the fatigue and corrosion behaviour of CFRP metal fastenings. Figure 4a represents the schematic of the fastening consisting of carbon fiber reinforced polymer (CFRP) sheet material with integrated metallic blind rivet nut (BRN). Blind rivet nuts are used to connect multiple CFRP fabrics and the joining of other components by bolting, so additional components such as coarse thread bolts are no longer required. The influence of plant force, applied for joining of the fastenings, on the fatigue behaviour of the fastening was investigated. Based on pull-out and torsion tests, the process window was confined to the plant force of minimum (min), maximum (max), and normal (norm).

In force-controlled stepwise load increase tests with load ratio R = -1 and frequency f = 10 Hz, the force amplitude starting from $F_{a,start}$ = 100 N was increased by ΔF_a = 100 N in each step after $\Delta N = 10^4$ load cycles until failure. The development of displacement amplitude s_a as a material response to the force amplitude F_a was recorded throughout the load cycles (Figure 4b), and evaluated taking into account the load steps as well as plant force (Figure 4c), in order to develop a relationship between plant force and fatigue behaviour.

At constant force amplitude, change in displacement amplitude Δs_a was interpreted as a signal of damage in the CFRP-metal fastening. The plot of the change in displacement per step as a function of plant force shows that initial damage as well as damage development depends upon the level of plant force. The specimens with minimum plant force show initial damage at F_a = 600 N, whereas those with maximum plant force at 700 N. The best results were achieved with a normal plant force, where the initial damage was detected earliest at F_a = 800 N. By further increasing force amplitude, a comparable exponential damage accumulation is observed, suggesting that this development is almost independent of the load level leading to initial damage caused by plant force.

During project progression, the corrosion behaviour of the material combinations CFRP aluminium and CFRP steel was investigated using electrochemical testing procedure – potentiodynamic polarization and immersion [15, 16]. While aluminium blind rivet nuts have high susceptibility to corrosion (Figure 4d), the corrosion resistance is understandably improved by applying stainless steel blind rivet nuts with CFRP sheet material.

Newly Developed Magnesium Alloy DieMag422 (Mg-4Al-2Ba-2Ca). The newly developed magnesium alloy DieMag422 contains nominally 4 wt.-% aluminium, 2 wt.-% barium and 2 wt.-% calcium. Scanning electron microscope (SEM) images (Figure 5a,

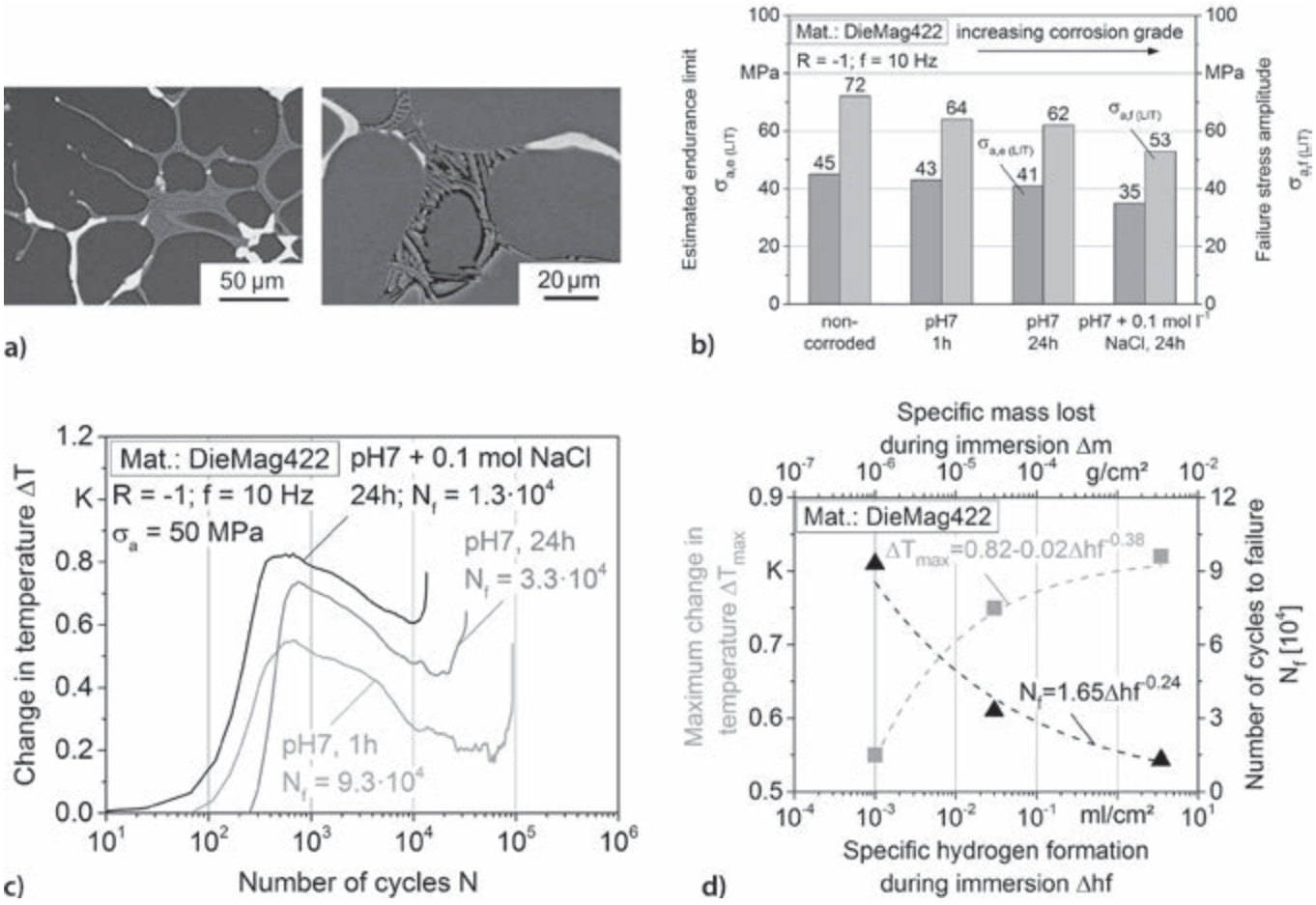

Figure 5. Results for the magnesium alloy DieMag422, a) microstructure in initial state (left) and after corrosion treatment (right), b) estimated endurance limit and determined failure stress amplitudes in continuous load increase tests as function of corrosion state, c) cyclic deformation curves based on change in deformation-induced temperature measurements in singe step tests, d) model-based correlation between fatigue and corrosion values

left) and EDX studies show that the grain boundaries of the primary α-Mg phase separates a compact Ba-rich phase (area fraction approx. 5.0 %) and a lamellar Ca-rich phase (area fraction approx. 10.8 %). Potentiodynamic polarization measurements show a selective corrosive attack between the α-Mg phase and the lamellar Ca-rich phase (Figure 5a, right) [15, 16].

Endurance limit at 2×10^6 cycles was estimated based on the material reactions plastic strain amplitude $\varepsilon_{a,p}$, change in deformation-induced temperature ΔT and change in electrical resistance ΔR measured in continuous load increase tests with a starting stress amplitude of $\sigma_{a,start} = 10$ MPa and a cycle dependent stress amplitude increase of $d\sigma_a/dN = 8\ MPa/10^4$ at load ratio R = -1 and frequency f = 10 Hz. Figure 5b shows the estimated endurance limit $\sigma_{a,e\ (LIT)}$ (left y-axis) and the fracture-inducing stress amplitude $\sigma_{a,f\ (LIT)}$ (right y-axis) for the base material (non-corroded) and the investigated corrosion conditions pH7 for 1 hour, pH7 for 24 hours, and pH7 + 0.1 mol l^{-1} NaCl for 24 hours.

For estimation of the endurance limit in load increase tests, the progression of the material response values was approximated asymptotically referring to the determination of the corrosion current density on the basis of anodic and cathodic branches by means of Tafel lines [11, 15, 16]. The estimated endurance limit $\sigma_{a,e\ (LIT)}$ decreased from 45 MPa in non-corroded state to 43 MPa after 1 hour in pH7. After 24 h in 0.1 mol l^{-1} NaCl solution it decreases about 22 % to 35 MPa. The fracture-inducing stress amplitude $\sigma_{a,f\ (LIT)}$ shows a similar tendency with increasing corrosion grade. After 1 h in pH7 it decreases from 72 MPa about 11 % to 64 MPa. In 0.1 mol l^{-1} NaCl solution it decreases about 26 % to 53 MPa. The quotient between estimated endurance limit $\sigma_{a,e\ (LIT)}$ and failure stress amplitude $\sigma_{a,f\ (LIT)}$ is about 66 % for all corrosion conditions.

Subsequently, the stress amplitude $\sigma_a = 50$ MPa was selected for investigating the comparative influence of the corrosion grades on the cyclic deformation behaviour and the lifetime in single step tests with load ratio R = -1 (Figure 5c). ΔT-N curves show a pronounced cyclic softening and hardening behaviour after an initial incubation period with ΔT nearby zero values. In comparison to the fatigue life at minimum corrosion level (1 h in pH7), the strongest corrosion level (24 h in pH7 + 0.1 mol l^{-1} NaCl) shows an 86 % decrease resulting in a lifetime of $N_f = 1.3 \times 10^4$ cycles, where a maximum ΔT increase of 0.8 K was observed. Increasing corrosion level results in increasing deformation values and in decreasing fatigue life.

In Figure 5d the qualitative relation between the characteristic fatigue and corrosion values is presented and quantitatively described in terms of understanding the basic structure property relationship for corrosion influence on fatigue performance of DieMag422 (Mg-4Al-2Ba-2Ca). For this purpose, the maximum change in temperature ΔT_{max} and the number of cycles to failure N_f determined in the single step tests (Figure 5c) are plotted as functions of the immersion test parameters specific mass loss Δm and specific hydrogen formation Δhf, respectively. Both characteristic values, Δm and Δhf, represent the corrosion state. With increasing corrosion degree the maximum temperature change increases according to $\Delta T_{max} = 0.82 - 0.02\Delta hf^{0.38}$ and the fatigue life decreases according to $N_f = 1.65\ \Delta hf^{0.24}$.

Magnesium Stent Tubules of Mg-10Gd-1Nd in Simulated Body Fluid (SBF). Biodegradable magnesium stents are increasingly used in medical applications because of dissolving in human body and not requiring surgical removal. For material selection and design of stents, accurate knowledge of their fatigue behaviour in corrosive media, as close as possible to human blood, is essential. In this context, magnesium stent tubules made of Mg-10Gd-1Nd were investigated for their cyclic behaviour in air and serum similar to body fluid. Single step tests were carried out on a micro magnetic fatigue testing system with a maximum force of 500 N. For fatigue tests in corrosive environment, a special miniature corrosion chamber was self-developed and integrated to the fatigue testing system (Figure 6a).

Figure 6b shows the Woehler curves representing the results of single step fatigue tests at load ratio R = 0.1 and frequency f = 20 Hz conducted in air at ambient temperature and in SBF environment at 37 °C body temperature. It is evident that in a corrosive atmosphere the stent tubules have a significant decrease in the sustainable maximum stress σ_{max} and fatigue life N_f, respectively. In air the maximum stress $\sigma_{max} = 110$ MPa ($\sigma_a \approx 50$ MPa) can be considered as the fatigue limit at 10^7 cycles. Due to transition from type I to type II S-N

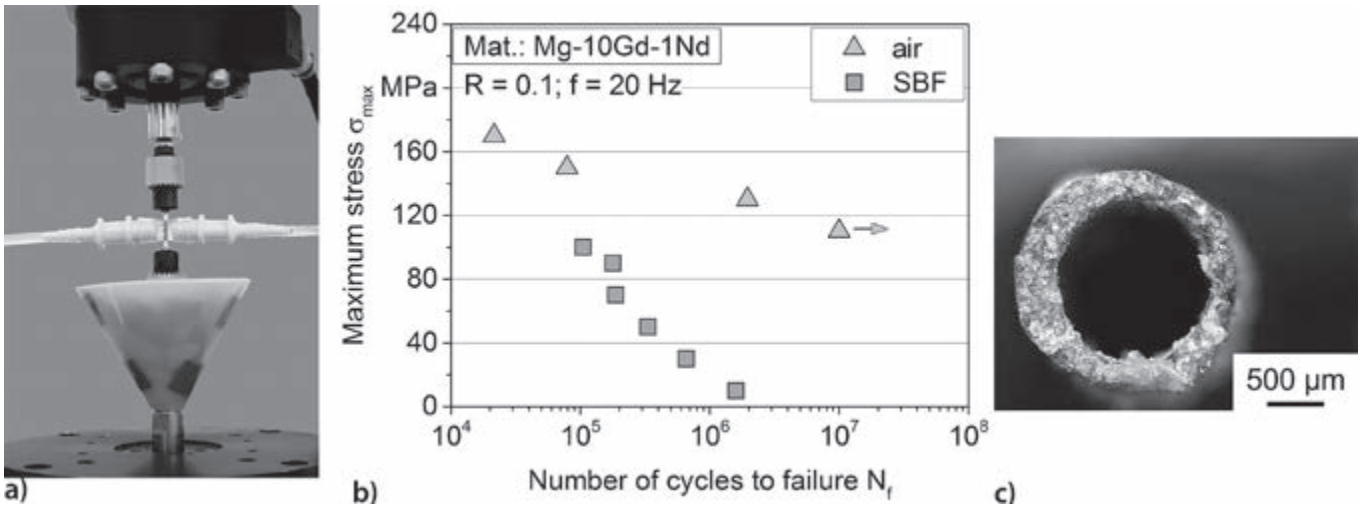

Figure 6. Illustrations for the magnesium stent tubule Mg-10Gd-1Nd, a) Experimental setup for corrosion fatigue tests in micro magnetic fatigue testing system, b) Woehler curves for air at ambient temp. and simulated body fluid at 37 °C, c) fracture surface after fatigue loading in simulated body fluid (SBF) with $\sigma_{max} = 30$ MPa

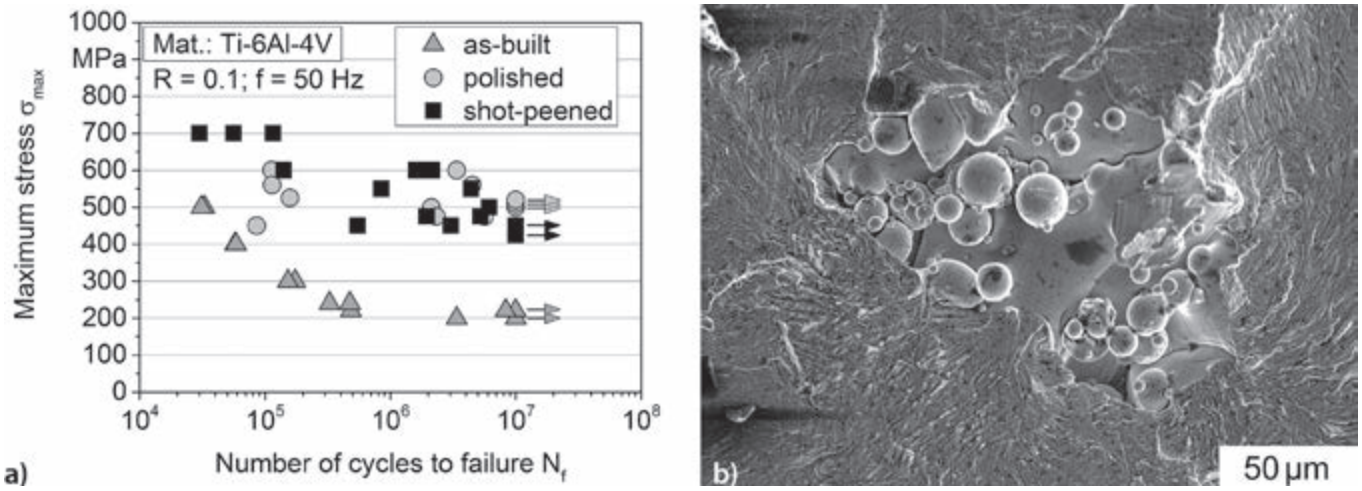

Figure 7. Test results for titanium alloy Ti-6Al-4V, a) Woehler curves for as-built, polished, and shot-peened specimens manufactured by selective laser melting (SLM), b) crack initiation at inner pores

curve, fatigue limit could not be determined in SBF environment even at lowest stresses investigated below 10 MPa. The determined parameters enable to qualify the investigated material in comparison to other biomaterials. Besides, an economical determination of the expected fatigue life in air and corrosive environment can be made.

Figure 6c shows the fracture surface of a stent tubule after a fatigue test in SBF with maximum stress σ_{max} = 30 MPa.

Selective Laser Melting of Titanium Alloy Ti-6Al-4V. Selective laser melting (SLM) is a novel additive manufacturing technique which uses laser energy for manufacturing in layer-wise pattern [17]. The SLM process offers a competitive advantage for manufacturing of complex and highly customized parts. The resulting quasi-static properties are comparable to those of conventionally manufactured components. The application of SLM components under cyclic loading has not yet been realized due to the lack of knowledge of their fatigue performance. However, the advantages of SLM manufacturing could be used for applications in aerospace and medical industry where titanium alloy Ti-6Al-4V is often used.

To investigate the fatigue performance of SLM manufactured Ti-6Al-4V specimens, single step tests were carried out for as-built, polished, and shot-peened conditions

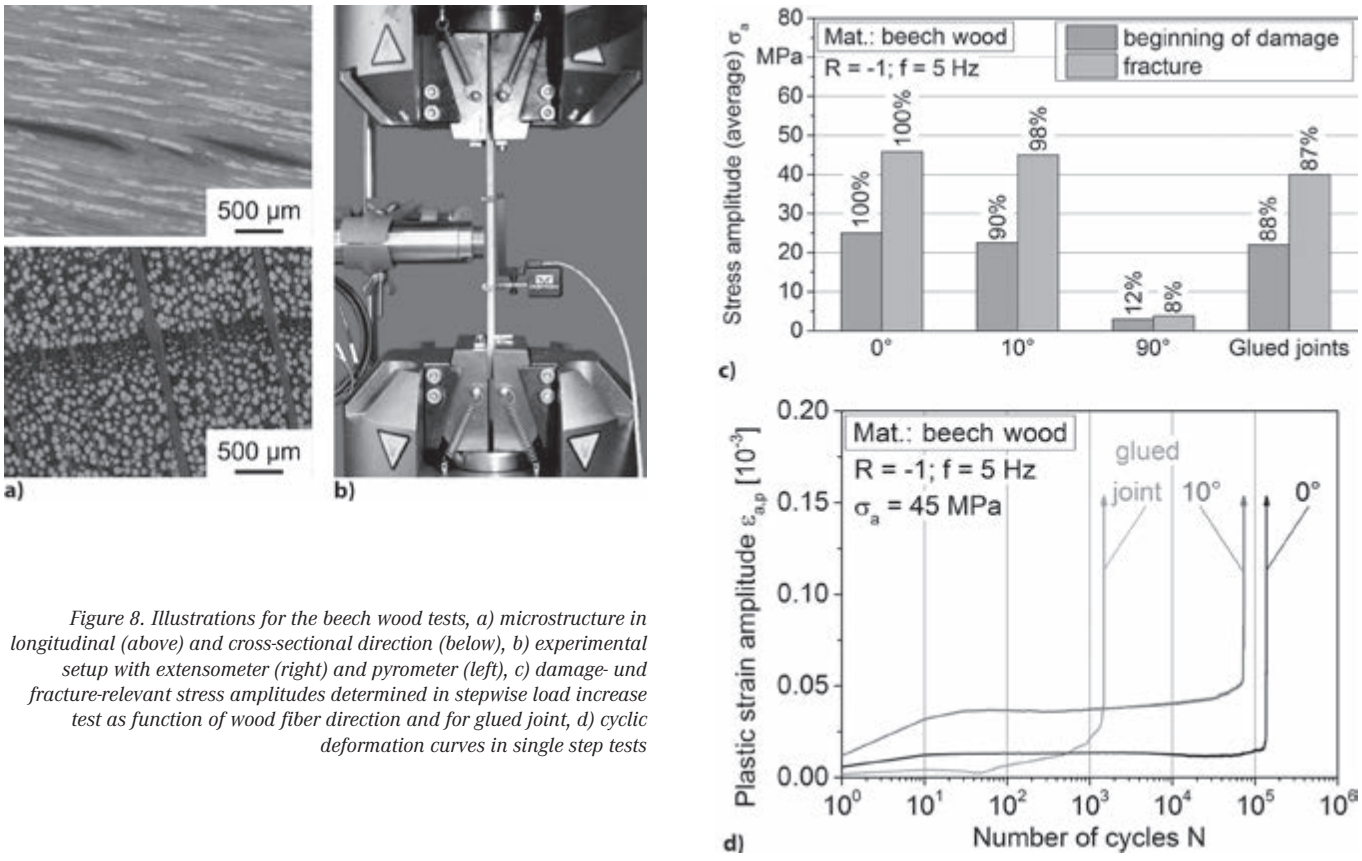

Figure 8. Illustrations for the beech wood tests, a) microstructure in longitudinal (above) and cross-sectional direction (below), b) experimental setup with extensometer (right) and pyrometer (left), c) damage- und fracture-relevant stress amplitudes determined in stepwise load increase test as function of wood fiber direction and for glued joint, d) cyclic deformation curves in single step tests

at load ratio R = 0.1 and frequency f = 50 Hz. In the Woehler curves (Figure 7a) the as-built specimens of SLM process result in a fatigue life σ_{max} = 210 MPa, almost 50 % of the fatigue life as compared to the conventionally manufactured alloy. This impaired performance is attributed to the high surface roughness ($R_a \approx 13$ µm) resulting from the SLM process. After polishing to $R_a \approx 0.8$ µm, the fatigue life increased to σ_{max} = 500 MPa. However, a high scatter in the fatigue life was observed which was attributed to multiple fatigue mechanisms revealed in the fracture analysis. In the specimens which failed after a small number of cycles, crack initiation occurred from inner pores which were found occasionally due to the fact that some powder material remained un-melted during the process (Figure 7b), whereas in the specimens which sustained the same stress until higher life cycles, a surface crack initiation was observed. Shot peening resulted in a slight impairment in the fatigue limit (σ_{max} = 435 MPa). Shot-peening is found detrimental to fatigue performance which is due to crack initiation from internal pores. Crack initiation occurring from pores of 30-40 microns or larger propagated very fast resulting in early failure.

Fiber Direction and Adhesive Bonding of Beech Wood Material. The determination of the fatigue behaviour of wood-based materials is relatively complex due to anisotropic properties. Beech wood is characterized by different fiber structures in longitudinal and cross-sectional directions as shown in Figure 8a.

After exceeding a material-dependent limit, cyclic loadings cause damage accumulating and leading to failure of the material. Stepwise load increase tests were carried out at load ratio R = -1 and frequency f = 5 Hz. The fatigue loading was started from a quasi-damage-free stress amplitude $\sigma_{a,start}$ = 2.5 MPa and was stepwisely increased by $\Delta\sigma_a$ = 2.5 MPa each $\Delta N = 10^4$ load cycles until failure. The material response was measured in terms of strain and temperature changes, yielding an indication of the initial damage and a prediction of the (remaining) lifetime. Since the fixation of thermocouples with adhesive tapes and adhesives bonded to the sample surface affects the fatigue results distinctly, a highly accurate pyrometer was used for these temperature measurements (Figure 8b).

The tests were conducted on flat samples at orientation of 0°, 10° and 90° to the fiber direction, and with Hysol 9492 (integrated with glass balls ∅ = 0.4 mm) glued lap joints. Figure 8c presents the load levels initial damage for the fiber directions and for the glued joint which was detected for and the load levels leading to failure in the load increase test. A significant decrease in fatigue strength of 90° specimens to 10 % compared to fatigue strength of 0° and 10° specimens is visible. The cyclic strength of the glued joint is about 10 % less than those determined in 0° fiber direction. These results were also verified in single step tests carried out at a stress amplitude σ_a = 45 MPa (Figure 8d).

The cyclic deformation behaviour, plotted in form of $\varepsilon_{a,p}$-N curves, is characterized by cyclic softening up to a saturation stage followed by secondary cyclic softening until failure. An increase in the stress amplitude from 45.0 MPa to 47.5 MPa leads to a reduction in fatigue life of about 70 % to 80 % [18].

Wood Polymer Composites (WPC). Owing to their good specific strength, wood and wood composite materials are in high focus, whereby wood polymer composites (WPC) play an important role. They possess good weather resistance compared to wood and have good formability characteristics like plastics. The fatigue behaviour of two types of WPC, 25 % PE matrix (Type A in Figure 9a, left) and 50 % PVC matrix (Type B in Figure 9a, right), have been investigated using load increase and single step tests. The results were compared to that of wood (beech, spruce) and vulcanized fiber [19], which serves as reference material in the range of technical plastics.

For the fatigue tests at load ratio R = -1 and frequency f = 5 Hz the specimens were instrumented with a mechanical extensometer for plastic strain measurements and thermocouples for change in temperature measurements (Figure 9b). The load increase tests were started at $\sigma_{a,start}$ = 2.5 MPa with a stepwisely increase of $\Delta\sigma_a$ = 2.5 MPa each $\Delta N = 10^4$ cycles. The single step tests were stopped at $N_{limit,SST} = 2 \times 10^6$ cycles.

In Figure 9c the endurance limit determined in single step tests (SST) $\sigma_{a,e\,(SST)}$ as left columns and the failure stress amplitude determined in stepwise load increase tests $\sigma_{a,f\,(LIT)}$ as right columns are plotted for the investigated wood and wood composite materials besides vulcanized fiber. Although the fatigue strength of vulcanized fiber is comparable to that of beech wood, spruce wood as well as both WPC types show a fatigue strength of about 20 % to 40 % for $N_{limit} = 2 \times 10^6$ cycles.

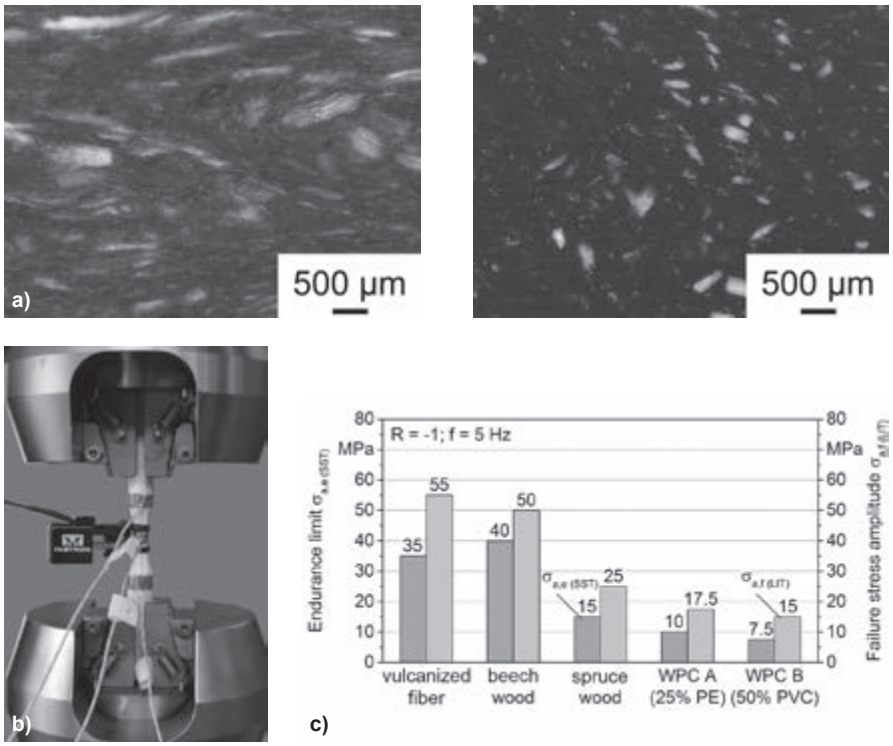

Figure 9. a) Microstructure of 25 % PE WPC (left) and 50 % PVC WPC (right), b) experimental setup with extensometer and thermocouples, c) endurance limits in single step tests and failure stress amplitudes in load increase tests for indicated materials

Summary

Mechanical, thermal and electrical measurement techniques are suitable for systematic microstructure-oriented fatigue assessment of metallic, polymer- and wood-based materials and joints under

multiple step and single step loading for the evaluation of the impact of joining technologies, environmental influences, and manufacturing processes. Plastic strain amplitude, deformation-induced change in specimen temperature and change in defect density leading to change in the resistivity measurements of the specimen can be effectively used.

Metrologically equipped stepwise and continuous load increase tests provide extensive information about the cyclic properties of investigated materials and fastenings using a small number of specimens in very short time. The rapid fatigue performance identification method based on load increase procedure can be applied for verifying the fatigue strength as a function of joining, environmental and manufacturing parameters in the context of in-process quality control. Due to time- and cost-efficient application it is very attractive for enterprises with the objective of a sufficient understanding of basic process structure property relationships, leading to a property-oriented production of tailored components with high fatigue resistance.

In addition to the applied mechanical, thermal and DC-based electrical measurement techniques, further magnetic and acoustic sensors are used in further research projects in the context of condition or structural health monitoring. Therefore, resistivity measurements based on AC current, Barkhausen noise and high frequency impulse (mechanical vibration) measurements are applied for structural integrity purposes, i. e., to improve the operational reliability of wind energy plants.

Acknowledgement

The author would like to thank the participating public funding institutions and industrial companies for their financial support of the projects, and project partners and colleagues for their excellent cooperation.

References

1 J. D. Morrow: Cyclic plastic strain energy and fatigue of metals, Internal Friction, Damping, and Cyclic Plasticity, 67th Annual Meeting ASTM, STP 378 (1964), pp. 45-87 DOI:10.1520/STP43764S

2 P. Lukáš, M. Klesnil: Cyclic stress-strain response and fatigue life in metals in low amplitude region, Materials Science and Engineering 11 (1973), pp. 345-356 DOI:10.1016/0025-5416(73)90125-0

3 H. Harig, E. Frank: Thermometry – a method of short term fatigue testing, Wire 31 (1981), No. 5, pp. 227-231

4 K. F. Stärk: Temperaturmessung an schwingend beanspruchten Werkstoffen, Zeitschrift für Werkstofftechnik 13 (1982), pp. 333-338 DOI:10.1002/mawe.19820131003

5 G. Meneghetti: Analysis of the fatigue strength of a stainless steel based on the energy dissipation, International Journal of Fatigue 29 (2007), pp. 81-94 DOI:10.1016/j.ijfatigue.2006.02.043

6 J. H. Constable, C. Sahay: Electrical resistance as an indicator of fatigue, IEEE Transaction on Components, Hybrids, and Manufacturing Technology 15 (1992), No. 6, pp. 1138-1145 DOI:10.1109/33.206940

7 M. Kocer, F. Sachslehner, M. Müller, E. Schafler, M. J. Zehetbauer: Measurement of dislocation density by residual electrical resistivity, Materials Science Forum 210-213 (1996), pp. 133-140 DOI:10.4028/www.scientific.net/MSF.210-213.133

8 D. D. L. Chung: Structural health monitoring by electrical resistance measurement, Smart Materials and Structures 10 (2001), pp. 624-636 DOI:10.1088/0964-1726/10/4/305

9 B. Sun, Y. Guo: High-cycle fatigue damage measurement based on electrical resistance change considering variable electrical resistivity and uneven damage, International Journal of Fatigue 26 (2004), pp. 457-462 DOI:10.1016/j.ijfatigue.2003.10.004

10 D. Dengel, H. Harig: Vergleich verschiedener Laststeigerungsverfahren zur Abschätzung der Dauerfestigkeit von Stahl, Materialprüfung 22 (1980), No. 3, pp. 120-130

11 F. Walther, D. Eifler: Cyclic deformation behaviour of steels and light-metal alloys, Materials Science and Engineering A 468-470 (2007), pp. 259-266 DOI:10.1016/j.msea.2006.06.146

12 F. Walther, D. Eifler: Fatigue life calculation of SAE 1050 and SAE 1065 steel under random loading, International Journal of Fatigue 29 (2007), No. 9-11, pp. 1885-1892 DOI:10.1016/j.ijfatigue.2007.01.005

13 F. Walther: Physikalische Messverfahren zur mikrostrukturbasierten Charakterisierung des Ermüdungsverhaltens und zur Lebensdauerberechnung metallischer Werkstoffe, D. Eifler (Ed.): Werkstoffkundliche Berichte, Vol. 19 (2008), pp. 1-180

14 M. Manka, L. Wojarski, W. Tillmann, G. Frieling, S. Myslicki, F. Walther: Fatigue behaviour of brazed AISI 304 joints using Au-fillers, Proc. of Loet 2013 – 10th Int. Conf. on Brazing, High Temperature Brazing and Diffusion Bonding, Aachen, DVS-Bericht Vol. 293 (2013), pp. 232-236

15 M. Klein, P. Wittke, H. Dieringa, F. Walther: Influence of corrosion on fatigue properties of new creep-resistant magnesium alloy DieMag422, Proc. of the 7th International Conference on Low Cycle Fatigue (2013), pp. 319-324

16 P. Wittke, M. Klein, F. Walther: Chemisch-mechanische Charakterisierung der kriech-

Abstract

Mikrostrukturbasierte Bewertung der Ermüdungsfestigkeit von Konstruktionswerkstoffen und Verbindungen mittels Kurzzeit-Laststeigerungsverfahren. Zur detaillierten Charakterisierung der unter Ermüdungsbeanspruchung auftretenden strukturmechanischen Prozesse wurden Messungen der Spannungs-Dehnungs-Hysterese, der verformungsinduzierten Temperaturänderung und der elektrischen Widerstandsänderung in mehrstufigen und einstufigen Untersuchungen angewendet. Ergebnisse des Einflusses der Verbindungstechnologie auf austenitischen Stahl X5CrNi18-10, kohlenstofffaserverstärkte Kunststoffe (CFK) und Buchenholzwerkstoffe, des Umgebungsmediums auf die Magnesiumlegierungen Mg-Al4-Ba2-Ca2 (DieMag422) und Mg-Gd10-Nd1 sowie des Herstellungsverfahrens auf die Titanlegierung Ti-Al6-V4 und auf Holz-Kunststoff-Verbundwerkstoffe (WPC) werden hier diskutiert. Die beanspruchungs- und lastspielzahlabhängige Veränderung der Mikrostruktur wurde licht- und elektronenmikroskopisch untersucht und mit den Ermüdungseigenschaften korreliert, um eine möglichst präzise qualitative und quantitative Beschreibung der Prozess-Struktureigenschafts-Beziehung zu erzielen. Das zeiteffiziente Laststeigerungsverfahren ist für den produktionsbegleitenden Einsatz zur Beurteilung von Verbindungstechnologien, Umgebungsmedien und Herstellungsverfahren auf die Ermüdungseigenschaften sehr gut geeignet.

beständigen bariumhaltigen Mg-Al-Ca-Legierung DieMag422, Materials Testing 56 (2014), No. 1, pp. 16-23 DOI:10.3139/120.110519
17 E. Wycisk, C. Emmelmann, S. Siddique, F. Walther: High Cycle Fatigue (HCF) Performance of Ti-6Al-4V Alloy Processed by Selective Laser Melting, Advanced Materials and Research 816-817 (2013), pp. 134-139 DOI:10.4028/www.scientific.net/AMR.816-817.134
18 S. Myslicki, T. Vallée, F. Walther: Short-term procedure for fatigue assessment of beech wood and adhesively bonded beech-joints, Wood Science and Technology (2014), submitted
19 B. Penning, F. Walther, D. Dumke, B. Künne: Einfluss der Verformungsgeschwindigkeit und des Feuchtegehalts auf das quasistatische Verformungsverhalten technischer Vulkanfiber, Materials Testing 55 (2013), No. 4, pp. 276-284 DOI:10.3139/120.110435

Bibliography

DOI 10.3139/120.110592
Materials Testing
56 (2014) 7-8, pp. 519-527

ISSN 0025-5300

The Author of This Contribution

Prof. Dr.-Ing. Frank Walther, born in 1970, studied Mechanical Engineering with specialization in materials science and engineering at TU Kaiserslautern, Germany, from 1992 to 1997 and finished his PhD on the fatigue assessment of highly-loaded ICE wheel steels at Institute of Materials Science and Engineering (WKK) in 2002. From 2002 to 2008 he was group leader of fatigue behaviour at WKK and finished his postdoctoral qualification (habilitation) in materials science and engineering in 2007. After that he joined Schaeffler AG in Herzogenaurach, Germany. Within corporate development he took responsibility for public private partnership concerning public research funding and special projects in materials research. Since December 2010 he has been professor of Materials Test Engineering (WPT) in the Faculty of Mechanical Engineering at TU Dortmund, Germany. His research portfolio includes determination of structure-property-relationships of construction materials and components taking the influence of manufacturing, joining and corrosion processes as well as service loading into account. New measurement and destructive/non-destructive testing techniques are applied for the characterization of fatigue behaviour from LCF to VHCF range under mechanical, thermal, chemical and mixed influences, as well as new physically based approaches for the calculation of damage development and (remaining) fatigue life.